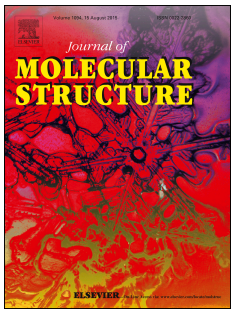

Water mediated procedure for preparation of stereoselective oximes as inhibitors of MRCK kinase

Manoj Kumar Shrivash, Shilipi Singh, Akhilesh Kumar Shukla, Suaib Luqman, Jyoti Pandey, Krishna Misra

PII: S0022-2860(20)31024-3

DOI: https://doi.org/10.1016/j.molstruc.2020.128699

Reference: MOLSTR 128699

To appear in: *Journal of Molecular Structure*

Received Date: 17 April 2020

Revised Date: 3 June 2020

Accepted Date: 11 June 2020

Please cite this article as: M.K. Shrivash, S. Singh, A.K. Shukla, S. Luqman, J. Pandey, K. Misra, Water mediated procedure for preparation of stereoselective oximes as inhibitors of MRCK kinase, *Journal of Molecular Structure* (2020), doi: https://doi.org/10.1016/j.molstruc.2020.128699.

Credit Author Statement

I hereby declare that the manuscript is being sent with the consent of all authors.There is no conflict of interest amonst the authors.

Krishna Misra

Graphical abstract:

Water Mediated Procedure for Preparation of Stereoselective Oximes as Inhibitors of MRCK Kinase

Manoj Kumar Shrivash, Shilipi Singh , Akhilesh Kumar Shukla, Suaib Luqman, Jyoti Pandey and Krishna Misra

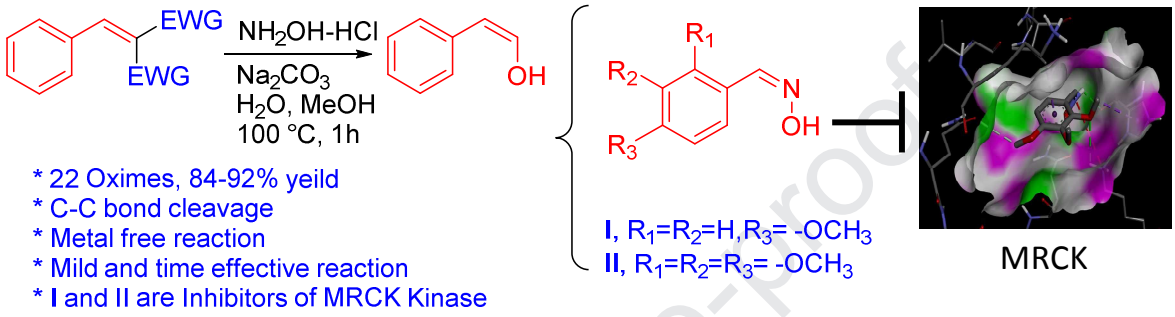

Water Mediated Procedure for Preparation of Stereoselective Oximes as Inhibitors of MRCK Kinase

Manoj Kumar Shrivash,[ab] Shilipi Singh [c], Akhilesh Kumar Shukla[b], Suaib Luqman[c], Jyoti Pandey[b] and Krishna Misra*[a]

[a]Centre of Biomedical Research, SGPGIMS, Campus Lucknow, 226014, India.

[b]Department of Applied Chemistry, Babasaheb Bhimrao Ambedkar University, Lucknow 226025, India

[c]CSIR-Central Institute of Medicinal & Aromatic Plants, Lucknow-226015, India.

*Corresponding email: krishnamisra4@gmail.com

ABSTRACT

Stereoselective aldoximes, preferably Z form have been obtained from α-cyano substituted carbonyl conjugated alkenes. This reaction occurs through Michael addition type reaction followed by retro-Knoevenagel reaction without transition-metal catalysis via C−C bond cleavage. These oximes are evaluated against cancer cell lines employing mechanistic study. Two oximes showed significant cytotoxic activity, which through in silico studies were found to inhibit MRCK Kinase, responsible for metastatic spread of cancer mortality.

Keywords: Stereoselective synthesis; Z-oximes; C-C bond cleavage, Retro-Knoevenagel reaction; MRCK kinase; Cancer cell lines

1. Introduction

Non-metallic catalytic C-C cleavage appears impossible because of the high energy block. The cleavage of carbon-carbon bond is a significant issue in organic chemistry due to its inert nature [1]. Although, the importance of the C−C bond cleavage has already resulted in different methodologies for the cleavage of C−C, C=C, and carbon-carbon triple bond [2-4]. The development of new routes for selective cleavage of C−C bond still remains an important and challenging goal for the chemists and biologists. The breaking of C-C bond with transition-metal complex is often studied [5]. In this regard, C-C bonds that are activated followed by transformation offer an attractive alternative approach in terms of disconnecting atoms, forming more active linkages, and producing more versatile scaffolds [6]. Stereoselective oximes are significant intermediates in organic synthesis [7-8]. The oximes can either be dehydrated to

nitriles [9] or converted to amides via an acid catalyzed Beckmann rearrangement [10]. Oximes are also key to ligands in the formation of mono- and poly metal complexes [11]. Oximes are used for protection, purification [12] and characterization of carbonyl compounds [13]. Moreover, oximes have been widely used in medicine, industry, and analytical chemistry [14-18]. The previously reported method for the synthesis of oximes is the reaction of a carbonyl compound with hydroxylamine hydrochloride in the presence of base (Scheme 1) [19-20]. However, this method has some drawbacks which restrict its further application. Recently, other studies have been achieved to obtain oximes via the redox methods under oxidation or reduction conditions [21] e.g .aerobic oxidation of primary amines by using 1,1-diphenyl-2-picryl-hydrazyl and tungstated alumina [22-25]. Some workers have reported the synthesis of oximes via oxidative ammoniation of carbonyl compounds [26-27]. However, these methods have more short-comings such as harsh reaction conditions, toxic metal salts, low yields, which adversely affect the applications extensively for the synthesis of oximes.

Scheme1: Conventional methods of synthesis of oximes yielding mixture of *E* & *Z* isomers and present method yielding predominantly *Z* isomer respectively.

The catalytic oxidation of amines is of major importance from both bioorganic and synthetic processes [28-29]. However, beneficial methods for catalytic oxidation are restricted, because of the sensitivity of amines. We report herein the first example where alkenes-bridged with electron-withdrawing groups undergo C-C bond cleavage with the concomitant loss of the specific group by Michael addition type reaction followed by retro Knoevenagel reaction. This method uses a weak base, water and methanol thus avoiding the use of DMF or NMP, which are expensive and difficult to remove from reaction mixture [30].

Our research group has now developed the synthesis of oximes, through direct conversion of aryl/alkyl cyano ester to aryl/alkyl oximes. The alkene-bridged ethyl cyano aryl acrylate compounds undergo C-C bond cleavage with the associated loss of the ethyl cyanoacetate group by Michael addition of hydroxylamine to a benzylidene cyanoacetate followed by a retro Knoevenagel reaction (1, 3 proton shift) without transition-metal catalysis. Besides this, the significant advantage of the present method is the formation of stereoselective oximes (Mainly *Z* –form) since this form is known to be biologically active (Scheme 1). The utility of

this method is seen not only in the synthesis of stereoselective substituted aryl/alkyl oximes but other styrene derivatives of commercial utility also by using different compatible nucleophiles. In recent years, there has been an increasing interest in the application of oximino group for enhancing the biological activity in a large variety of molecules. In Steroids oximino group is well known for its anticancer properties [31]. The oxime derivatives of curcumin show strong antiproliferative activity against some cancer cell lines. Besides, the efficacy of these compounds in reversing the efflux-mediated resistance developed by cancer cells has also been studied [32]. It is reported that the oxime derivatives of 1, 4-naphthoquinone exhibited higher cytotoxic activity against cancer cells MDA-MB-231 and (HSF), but lower cytotoxic activity against normal cell [33]. 5-Nitro, 5- flouro-indirubin-3-oxime showed antiproliferative activity against human cancer cell line [34]. α, β- unsaturated oximes have exhibited high antiproliferative activity against (Panc-1), (A-549), (PaCa-2) and (PC-3) cell lines [35] Quinazolinone was inactive against nasopharyngeal carcinoma (NPC-TW01), lung carcinoma and leukemia while quanozolinone oxime and quanozolinone methyl oxime exhibited more potent antiproliferative activity [36]. The two structurally related protein kinase families, the Rho kinases (ROCK) and themyotonic dystrophy kinase-related Cdc-binding kinases (MRCK) are required for migration and invasion of cancer cells [37]. These regulate the assembly and organization of the actin cytoskeleton in all eukaryotic cells and have been the center of much attention in cancerous growth and metastatic [38]. It has been reported that MRCK inhibition was adequate to decrease invasion by squamous cell carcinoma cells [39-41].

Simultaneous targeting of these two kinase families is likely to block the migration and invasion of metastatic cancers. If inhibition of ROCK and MRCK kinases has a greater effect in preventing cancer spread motility and local invasion, highly selective small-molecules of oximes may act as inhibitors, thus proving useful for prevention of tumor invasion and metastasis. We have designed and prepared eighteen *Z*-oximes, out of which two have shown high activity against all the nine different cancer cell lines.

2. Results and discussion

2.1 Synthesis of Z oximes (2a-2v)

In continuation of our materials research, we focused on the study of 2-Cyano-3-N-hydroxylamino-3-phenyl ethyl propionate (2). Methanolic solution of a benzylidene cyanoacetate (1) was treated with hydroxylamine hydrochloride in aqueous sodium carbonate solution (Scheme 3; Table 1, entry 7) to synthesize (2). Unexpectedly, benzyl oxime **2a** was formed because of the loss of the ethyl cyanoacetate moiety (Scheme 3). This structure was confirmed by using IR spectra, ^{1}H NMR, ^{13}C NMR spectrum. The other expected products as shown in (Scheme 2) were also not detected. A preliminary examination of the impact of solvents on reactions shows that the oxime (**2a**) is obtained as the major product with most of the alcoholic solvents used. Perhaps surprisingly, using water (Table 1, entry 7) it was obtained as the major product. With an increase in reaction temperature to 100 °C, for 1h only (**2a**) was isolated. A chemical reaction involving loss of ethyl cyanoacetate group by C−C bond cleavage, by the Michael type addition of hydroxylamine hydrochloride has not been reported previously. Another example of ethyl cyanoacetate group loss was observed when aqueous hydroxylamine hydrochloride was reacted with other similar substrates (Scheme 4-5).The screening of different solvents revealed that the solvent plays an important role in this reaction. Particularly, methanol: water (9:1) was the only efficient solvent for the formation of oximes, while no reaction occurred in other solvents (Table 1, entries, 1–6). Moreover, the effect of the reaction temperature was also examined, and it was found that a temperature of 100 °C was optimal for this reaction (Table 1, entries, and 7–12). Although methanol: water (9:1) was the best choice for this reaction, other solvents such as ethanol: water and DMSO: water were also effective, however affording the products with slightly reduced yields (Table 1, entries 8–12).

Scheme 2: Formation of oxime due to C-C bond cleavage.

Table 1: Optimization of the reaction conditions

Scheme 3: Unexpected formation of benzyl oxime (2a)

Scheme 4: Benzyl oxime (2a) from benzylidene malononitrile.

The Screening of various bases as catalysts (Table 2, entries,1-7) show that these play an important role in this reaction. With the increase of pKa value yield of (2a) decreased (Table 2, entries, 1-7) therefore sodium carbonate and potassium carbonate gave better conversion of

stereoselective oximes. Further optimization of the results showed that optimum amount of base i.e. 1.1 equivalent gave (Table 2, entries 1–7) excellent yield. Additionally, the reaction was less efficient while proceeding in only water (Table 1, entry 12). The scope of reaction was assessed by using other substrates under similar conditions (Scheme 4-5) to yield corresponding stereoselective oximes (*Z*-isomer) followed by carbon–carbon bond cleavage. With the optimized conditions in hand, we turned our attention to the scope of the reaction. As summarized in (Table 3), a variety of ethyl cyanoaryl acrylates were converted to corresponding oximes. The reaction could be successfully applied to a range of different substituted substrates yielding the corresponding oximes in almost excellent yields. Ethyl cyanoaryl acrylates with either electron donating or electron-withdrawing groups on the benzene ring smoothly generated the corresponding products, however in varying yields Electronic effects play an important role, as electron-withdrawing substituents (Table 3, **2p**) on the benzene ring favored the transformation. Meanwhile, electron-donating substituents (Table 3, entries **2b–2h**, and **2n, 2o**) hindered the transformation. This is evident from the mechanism given in (Scheme 1), since electron-withdrawing groups will facilitate nucleophilic attack at α-position. The ethyl (*E*)-2-cyano-3-(4-methoxyphenyl) acrylate substrate gave the two isomeric products, i.e. *E* isomer oxime and *Z* isomer oxime in 90:10 ratio. Both isomers were confirmed by melting points and ^{1}HNMR Spectrum.

Scheme 5: Benzyl oxime (**2a**) from dimethyl-2-benzylidene malonate.

Table 2: Impact of base on yield of benzyl oxime.

Additionally, the reaction conditions were also compatible with fluoro, chloro, and bromo substituents (Table 3, entries **2j–2l**). The yield was excellent in case of fluorine being in the para position of benzene followed by bromine in the same position. With chlorine at either ortho or meta positions (Table 3, entries **2k** and **2l**), the yield was slightly lower than fluoro /bromo derivatives. This may be due, in part, to steric hindrance. Ethyl (E-2-cyano-3-(naphthalen-1-yl) acrylate could also be successfully converted into the corresponding oximes in good yields (Table 3, **2i**). Moreover, we also conducted the reaction with heterocyclic substrates under the optimized reaction conditions (Table 3, **2s**), with good yields.

Scheme 6: Control experiment.

Table 3: Substrate scope of *Z* oximes.

Scheme 7: a plausible mechanism is proposed for the synthesis of benzyl oxime (**2a)**.

Surprisingly, in the case of ethyl (E)-2-cyano-3-(1H-indole-3yl) acrylate, a heterocyclic derivative an equivalent yield of oxime was obtained (Table 3, **2s**). However, the yield in the case of aliphatic oximes was quite low (See table 3; **2t, 2u, 2v**). To demonstrate the scope and efficiency of the present method, this mild system was then extended for the synthesis of aliphatic oximes. However, we found that the heptyl substrate (Table 3, **2r**) did react and gave very low conversion and amount of yield. To check the viability of ethyl cyanoacetate as leaving group, we also replaced it with malononitrile and dimethylmalonate groups. Using optimized reaction conditions we found that both these groups gave comparable yields of benzyl oxime (Scheme 4-5). To assess the effect of electron-withdrawing group we used one EWG in place of two and observed that C-C cleavage did not take place and no oxime was formed. The role of water was also assessed and the exclusion of water also resulted in the non-formation of oxime. Experiment with ethyl cinnamate which has only one EWG when reacted with aq. hydroxyl amine in methanol at 100 °C for 1h we did not find benzyl oxime (**2a**), rather N-hydroxycinnamamide was formed, therefore one electron withdrawing group did not leave from the substrate as shown in (Scheme 6). The presence of two EWG i.e cyano and ester groups gave the oxime as shown in (Scheme 7). Based on the above control experiments (,a plausible mechanism is proposed for the synthesis of **2a** (Scheme 7). Firstly, the reaction of ethyl (E)-2-cyano-3-phenylacrylate with hydroxylamine catalyzed by Na_2CO_3 give a Michael addition product as an intermediate. Then a retro Knoevenagel reaction is taken place through attacked base on intermediate (1, 3 proton shift) and subsequent carbon-carbon bond cleavage to give the final product **2a**. The mechanism shown explains the formation of Z-isomer preferentially since the heavier leaving group orients the preferable configuration (scheme 7).

3. Biological activities

3.1 Anticancer activity of synthetic oximes (MTT Assay)

Among all the twenty two synthesized compounds, **2g** (2, 3, 4-trimethoxy benzyl oxime) showed maximum growth inhibition in all the tested cancer cell lines (range of IC_{50} 9.42 ± 0.39-18.75 ± 3.39 µg/mL) but it also showed moderate toxicity for normal cell line (L-132) with an IC_{50} value of 44.26 ± 0.39 µg/mL (Table 4). Compound **2d** (*p*-methoxy benzyl oxime) showed toxicity against all the tested cancer cell lines (range of IC_{50} 8.63 ± 0.15-23.84 ± 0.50 µg/mL) as well as in normal cell line (IC_{50} 37.84 ± 1.27 µg/mL). Compound **2i** inhibits the growth of skin, lung and breast cancer cell lines (12.25 ± 0.40-24.49 ± 1.27 µg/mL) but slightly altered the growth of the squamous carcinoma and hepatic carcinoma with the percent inhibition of 43.23 ± 1.03 and 47.58 ± 3.68 respectively at the highest tested concentration (50µg/mL). It also showed toxicity against normal cell line (L-132) with an IC_{50} value of 28.69 ± 0.86 µg/mL whereas compound **2l** and **2k** selectively showed toxicity against the skin carcinoma (IC_{50} 40.80 ± 1.55 µg/mL) and breast carcinoma (IC_{50} 38.84 ± 0.70 µg/mL, (Table 4, Fig 1). Rest of the compounds altered the growth of cells feebly with the percent inhibition ranged from 14.31 ± 0.95-48.57 ± 5.47.

Table 4: IC_{50} value of synthesized compound for tested cell line.

Figure 1: Percent cytotoxicity of synthetic oximes (2b-2p) vs standard drug Tamoxifen.

3.2 Docking study of bioactive oximes against MRCK protein

The oxime moiety of the paramethoxy benzaldehyde oxime (**2d**) ligands provides binding site opening interacting with MRCK around the Gln 144, Val 35, Asp 32 and oxime moiety of tri methoxy benzaldehyde oxime (**2g**) interacted with MRCK Gln 144, Val 35, His 395, Lys 109, Gln 70. As well as binding energy of **2d**, **2g** respected -5.1 and -5.9 (Fig. 2). **2g** ligand interacted with MRCK kinase with good binding energy compared with **2d** and both ligand are inhibited cell invasion pathways of metastatic stage.

Figure 2: *(A) Interaction of **2d** with MRCK Kinase (3D); (B) Interaction of **2d** with MRCK Kinase (2D); (C) Interaction of **2g** with MRCK Kinase (3D); (D) Interaction of **2g** with MRCK Kinase (2D).*

3.3 Cell cycle analysis

Compound **2g** and **2d** at the inhibitory concentration (IC_{50}) and double the inhibitory concentration IC_{50} for 24 h altered the phases of the cell cycle. In A431 cell line, the compound **2g** slightly increased the apoptotic cells at both the tested concentration. Compound **2g** reduced

the G0/G1 phase up to 1.14 fold and increased the number of cells in S phase at both the concentration 10.24µg (1.1fold) and 20.48 (1.6 fold). There is a non-significant alteration was observed in the G2/M phase, whereas compound **2d** increased 1.1 and 1.2 fold number of cells in the G2/M phase at both the tested concentration, respectively. Compound **2d** at the concentration of 9.11 µg decreased the cells in S phase, but at the concentration of 18.22µg, it increased the 1.2 fold number of cells (Fig 3). The reduction of cells in G0/G1 phase was observed at both the concentration up to 1.3 fold. The compound **2d** showed up to 4.3 fold increased number of apoptotic cells in comparison to control. In NCIH-460 cell line, the number of apoptotic cells was increased 1.4 and 3.1fold at both the tested concentration respectively after the treatment with compound **2g**. Simultaneously, compound **2g** reduced the number of cells in G0/G1, S, and G2/M phase up to 2.4 fold.

Similarly, Compound 2d increased the apoptotic cells at the both tested concentrations 8.63 µg (3.2 fold) and 17.26µg (4.4 fold) and decreased the number of cells in G0/G1, S and G2/M phase up to 1.5 fold (Fig 4). From the results, we can interpret that the compound **2g** inhibit the cell proliferation of A431 cells by arresting the cell cycle in S phase, whereas in NCIH-460 cells by increasing apoptosis. The compound **2d** altered the cell growth of A431 cells by inducing apoptosis and G2/M phase arrest, but in NCIH-460 cells, the cell proliferation was inhibited by inducing apoptosis.

3.4 Apoptosis assay (Annexin-V-FITC)

Both the compound showed apoptosis in NCIH-460 cell line; therefore, we further performed the annexin-V assay to confirm the apoptosis at the two concentrations IC_{50} and Double of IC_{50}. Compound **2g** showed 0.7% and 8.25% late apoptosis, 1.8 % and 3.6 % necrosis at both the tested concentration, respectively (Fig 5). Compound **2d** showed 3% and 19.3% late apoptosis, 1.4 % and 2.6 % necrosis at both the tested concentration respectively.

3.5 Reactive oxygen species (ROS) estimation

Both the tested compounds increased the apoptosis in NCIH-460 cell line, and as earlier reports suggested that the ROS are involved in the apoptotic pathway46. Therefore, we further evaluate the ROS inducing effect in NCIH-460 cell line at the two concentrations IC_{50} and Double of IC_{50}. The results showed that the compound **2g** induced ROS formation (1.05 fold) only at the Double

of IC_{50} (17.26µg) whereas the compound 2d increased the ROS formation 1.2 fold and 1.6 fold at both the tested concentration respectively in comparison to control (Fig 6). The results indicated that the apoptotic potential of compound **2d** might be due to ROS production.

3.6 Mitochondrial membrane potential estimation

The mitochondrial membrane potential is also associated with the apoptotic pathway; therefore we also evaluated the effect on mitochondrial potential by using the rhodamine dye in NCIH-460 cell line at the two concentrations IC_{50} and Double of IC_{50}. The data showed that both the compounds **2g** and **2d** did not alter the mitochondrial membrane potential significantly (Fig 7). The finding suggests that the compounds did not use mitochondria-mediated apoptosis pathway for cell growth inhibition.

Figure 3: *The effect of compound **2g** and **2d** in the A431 cell line on different phases of the cell cycle. The cell cycle analysis was performed by using propidium iodide (PI) staining. The pictorial graphs and percent population graphs are presented, and the pictorial graphs are one representative example of two experiments.*

Figure 4: *The effect of compound **2g** and **2d** in NCIH-460 cell line on different phases of the cell cycle. The cell cycle analysis was performed by using propidium iodide (PI) staining. The pictorial graphs and percent population graphs are presented, and the pictorial graphs are one representative example of two experiments.*

Figure 5: *The apoptotic effect of compound **2g** and **2d** in NCIH-460 cell line. The apoptosis assay was performed by using Annexin-V-FITC staining. The pictorial graphs and percent population graphs are presented, and the pictorial graphs are one representative example of two experiments.*

Figure 6: *The ROS generation effect of compound **2g** and **2d** in NCIH-460 cell line. The reactive oxygen species (ROS) assay was performed by using DCFDA dye. The pictorial graphs and*

FITC mean graphs are presented, and the pictorial graphs are one representative example of two experiments.

Figure 7: *The effect of compound **2g** and **2d** on mitochondrial membrane potential in NCIH-460 cell line. The mitochondrial membrane potential (MMP) assay was performed by using Rhodamine 123 dye. The pictorial graphs and FITC mean graphs are presented, and the pictorial graphs are one representative example of two experiments.*

4.Experimental section

4.1 General

All chemicals used in these syntheses were purchased from Sigma-Aldrich, Fisher Scientific, Avra chemicals and used without further purification. Unless otherwise stated, all reactions were carried out without inert atmosphere of nitrogen, NMR spectra were recorded in $CDCl_3$, DMSO-D_6 with a Bruker Avance III spectrometer operating at 400 MHz and 800MHz, for ^1H spectra and 101 MHz and 201 MHz for ^{13}C spectra. ^1H and ^{13}C NMR spectra were referenced relative to TMS (δ = 0.00 ppm) ^{13}C NMR spectra were proton-decoupled. Chemical shifts (δ) are reported in ppm and coupling constants in Hz. Electro spray ionization (ESI) mass spectrometry (MS) experiments were performed on Agilent Technologies 6530Accurate-Mass QTOF LC/MS.

4.2. Chemistry

4.2.1 General Procedure for the Preparation of α, β-unsaturated Compounds (1a-1v).

A mixture of substituted aldehyde (10 mmol), ethyl cyanoacetate or malononitrile (10.1 mmol) and piperidine (20 mol %) in 25 ml ethanol was reflux at 80-85 °C for 4-8h and room temperature for 8-24h. The progress of the reaction was monitored by TLC. After completion of reaction, as monitored by TLC, the reaction mixture was directly charged onto silica gel column and eluted with a mixture of ethyl acetate: n-hexane to afford pure olefin. All the products were prepared by using the same procedure. The olefinic products thus obtained were characterized by comparison of their ^1H NMR, ^{13}C NMR spectroscopy and mass spectroscopic.

*4.2.2 General procedure for preparation of stereoselective oximes (**2a-2v**).*

To the stirred sodium carbonate (632 mg, 5.9 mmol), hydroxylamine hydrochloride (414mg, 5.9 mmol), water (2.5 mL), and the solution of substituted Ethyl (E)-2-cyano-3-phenylacrylate (4.9 mmol), methanol (22.5 mL) was added in the reaction mixture and refluxed for 1h. Reaction monitored with TLC, after completion of reaction, the mixture was concentrated under reduced pressure and the crude compound purified with column chromatography elution ingredients hexane: ethyl acetate.

4.2.2.1 (Z)-benzaldehyde oxime (2a). Isolation condition: Hexane: ethyl acetate (95:5), Yellow gel (556mg, 92%) ^{1}H NMR (400 MHz, $CDCl_3$) δ 8.76 (s, 1H), 8.17 (s, 1H), 7.60 – 7.54 (m, 2H), 7.41 – 7.36 (m, 3H).^{13}C NMR (101 MHz, $CDCl_3$) δ 150.42, 131.92, 130.13, 128.83, 127.08, 77.06, HRMS (ESI): Calculated for C_7H_7NO $[M+H]^+$: 122.0528, found 122.0600.

4.2.2.2 (Z)-4-hydroxybenzaldehyde oxime (2b). Isolation condition : Hexane: ethyl acetate (8:2), White solid (450mg, 83.9%), ^{1}H NMR (800 MHz, $DMSOD_6$) δ 10.83 (s, 1H), 9.73 (s, 1H), 7.99 (s, 1H), 7.39 (d, *J* = 8.6 Hz, 2H), 6.77 (d, *J* = 8.6 Hz, 2H). ^{13}C NMR (201 MHz, $DMSOD_6$) δ 159.00, 148.34, 128.41, 124.48, 116.00, 40.24, 40.14, 40.03, 39.93, 39.82, 39.72, 39.62, 38.02, HRMS (ESI): Calculated for $C_7H_7NO_2$ $[M+H]^+$: 138.0477, found 138.0532.

4.2.2.3 (Z)-3,4-dihydroxybenzaldehyde oxime (2c). Isolation condition : Hexane: ethyl acetate (5:5), White solid (401mg, 77%), ^{1}H NMR (400 MHz, $DMSOD_6$) δ 10.71 (s, 1H), 9.15 (s, 1H), 9.03 (s, 1H), 7.82 (d, *J* = 24.7 Hz, 1H), 6.97 (d, *J* = 1.9 Hz, 1H), 6.74 (dd, *J* = 8.2, 1.9 Hz, 1H), 6.66 (d, *J* = 8.1 Hz, 1H). ^{13}C NMR (101 MHz, $DMSOD_6$) δ 148.59, 147.40, 145.93, 124.91, 119.71, 115.98, 113.04, 40.52, 40.31, 40.11, 39.90, 39.69, 39.48, 39.27, HRMS (ESI): Calculated for $C_7H_7NO_3$ $[M+H]^+$: 154.0426, found 154.0459.

4.2.2.4 (Z)- 4-methoxybenzaldehyde oxime (2d).Isolation condition: Hexane: ethyl acetate (8:2), Pale yellow semi solid (550mg, 85.6%), ^{1}H NMR (400 MHz, $CDCl_3$) δ 9.25 (s, 1H), 8.11 (s, 1H), 7.53 – 7.48 (m, 2H), 6.92 – 6.87 (m, 2H), 3.81 (s, 3H) ^{13}C NMR (101 MHz, $CDCl_3$) δ 161.08, 150.02, 128.59, 124.59, 114.30, 77.09, 55.36, HRMS (ESI): Calculated for $C_8H_9NO_2$ $[M+H]^+$: 152.0633, found 152.0667.

4.2.2.5(Z)-3-methylbenzaldehyde oxime (2e).Isolation condition, Hexane: ethyl acetate (9:1), Transparent liquid (560mg, 89%), ^{1}H NMR (400 MHz, $CDCl_3$) δ 8.57 (d, *J* = 13.2 Hz, 1H), 8.43 (s, 1H), 7.68 – 7.64 (m, 1H), 7.28 (td, *J* = 7.4, 1.4 Hz, 1H), 7.24 – 7.17 (m, 2H), 2.43 (s, 3H). ^{13}C

NMR (101 MHz, $CDCl_3$) δ 149.30, 136.84, 130.87, 130.22, 129.88, 126.72, 126.27, 77.36, 77.05, 76.73, 19.77, HRMS (ESI): Calculated for C_8H_9NO $[M+H]^+$: 136.0685, found 136.0758.

4.2.2.6 (Z)-3,4-dimethoxybenzaldehyde oxime (2f). Isolation condition, Hexane: ethyl acetate (8:2), White solid (598mg, 86%),^{1}H NMR (400 MHz, $CDCl_3$) δ 8.55 (s, 1H), 8.11 (s, 1H), 7.24 (d, *J* = 1.9 Hz, 1H), 7.05 (dd, *J* = 8.3, 1.9 Hz, 1H), 6.89 – 6.86 (m, 1H), 3.92 (s, 6H). ^{13}C NMR (101 MHz, $CDCl_3$) δ 150.82, 150.24, 149.30, 124.82, 121.73, 110.76, 107.99, 77.39, 77.07, 76.75, 55.94, 55.89, HRMS (ESI): Calculated for $C_9H_{11}NO_3$ $[M+H]^+$: 182.0739, found 182.0802.

4.2.2.7 (Z)- 2,3,4-trimethoxybenzaldehyde oxime (2g). Isolation condition, Hexane: ethyl acetate (7.5:2.5), White crystalline solid (635mg, 88%), ^{1}H NMR (400 MHz, $CDCl_3$) δ 8.29 (s, 1H), 7.35 (d, *J* = 8.8 Hz, 1H), 6.63 (d, *J* = 8.8 Hz, 1H), 3.84 (s, 3H), 3.82 (s, 3H), 3.81 (s, 3H). ^{13}C NMR (101 MHz, $CDCl_3$) δ 155.29, 152.69, 146.29, 142.17, 121.45, 118.63, 107.88, 77.05, 61.72, 60.95, 56.08, HRMS (ESI): Calculated for $C_{10}H_{13}NO_4$ $[M+H]^+$: 212.0845, found 212.0917.

4.2.2.8 (Z)-4-hydroxy-3-methoxybenzaldehyde oxime (2h). Isolation condition, Hexane: ethyl acetate (7:3), pale yellow solid (550mg, 85%),^{1}H NMR (400 MHz, DMSO) δ 10.86 (s, 1H), 9.36 (s, 1H), 8.00 (s, 1H), 7.17 (d, *J* = 1.5 Hz, 1H), 6.98 (dd, *J* = 8.1, 1.6 Hz, 1H), 6.79 (d, *J* = 8.1 Hz, 1H), 3.78 (s, 3H). ^{13}C NMR (101 MHz, DMSO) δ 148.50, 148.42, 148.26, 124.88, 120.93, 115.89, 109.59, 55.89, 39.93, HRMS (ESI): Calculated for $C_8H_9NO_3$ $[M+H]^+$: 168.0582, found 168.0627.

4.2.2.9 (Z)-1-naphthaldehyde oxime (2i). Isolation condition, Hexane: ethyl acetate (8.5:1.5), Light green solid (600mg, 88%), ^{1}H NMR (800 MHz, DMSO) δ 11.49 (s, 1H), 8.79 (s, 1H), 8.67 (d, *J* = 8.4 Hz, 1H), 7.96 (t, *J* = 9.2 Hz, 2H), 7.80 (d, *J* = 7.0 Hz, 1H), 7.57 (ddd, *J* = 23.4, 15.1, 7.4 Hz, 3H). ^{13}C NMR (201 MHz, DMSO) δ 148.31, 133.49, 130.01, 129.73, 128.79, 128.66, 127.01, 126.93, 126.20, 125.56, 124.75, 39.62, 39.51, 39.40, HRMS (ESI): Calculated for $C_{11}H_9NO$ $[M+H]^+$: 172.0684, found 172.0745.

4.2.2.10 (Z)-4-fluorobenzaldehyde oxime (2j). Isolation condition, Hexane: ethyl acetate (9:1), White crystalline solid (580mg, 92%), ^{1}H NMR (400 MHz, $CDCl_3$) δ 8.12 (s, 1H), 7.82 (s, 1H), 7.60 – 7.53 (m, 2H), 7.12 – 7.04 (m, 2H) , ^{13}C NMR (101 MHz, $CDCl_3$) δ 165.06, 162.57,

149.30, 128.94, 128.86, 128.16, 116.09, 115.87, 77.35, 77.03, 76.71, HRMS (ESI): Calculated for C_7H_6FNO $[M+H]^+$: 140.0433, found 140.0490.

4.2.2.11(Z)-2-chlorobenzaldehyde oxime (2k). Isolation condition, Hexane:ethyl acetate (9:1), White crystalline solid(580mg, 88%),^{1}H NMR (400 MHz, $CDCl_3$) δ 8.58 (s, 1H), 8.31 – 8.22 (m, 1H), 7.82 (dd, *J* = 7.7, 1.8 Hz, 1H), 7.41 – 7.38 (m, 1H), 7.32 (ddd, *J* = 9.8, 5.7, 2.0 Hz, 1H), 7.29 – 7.24 (m, 1H). ^{13}C NMR (101 MHz, $CDCl_3$) δ 147.60, 133.97, 132.03, 131.01, 129.95, 129.81, 129.77, 127.16, 127.03, 126.55, 77.34, 77.03, 76.71, HRMS (ESI): Calculated for C_7H_6ClNO $[M+H]^+$: 156.0138, found 156.0192.

4.2.2.12 (Z)-3-chlorobenzaldehyde oxime (2l). Isolation condition, Hexane:ethyl acetate (9:1), White crystalline solid(581mg, 88%),^{1}H NMR (400 MHz, $CDCl_3$) δ 8.18 (d, *J* = 1.7 Hz, 1H), 8.10 (s, 1H), 7.59 (q, *J* = 1.6 Hz, 1H), 7.44 (dt, *J* = 7.3, 1.3 Hz, 1H), 7.36 (dt, *J* = 3.5, 1.5 Hz, 1H), 7.34 – 7.29 (m, 1H). ^{13}C NMR (101 MHz, $CDCl_3$) δ 149.19, 134.87, 133.75, 130.04, 126.85, 125.27, 77.35, 77.03, 76.71, HRMS (ESI): Calculated for C_7H_6ClNO $[M+H]^+$: 156.0138, found 156.0200.

4.2.2.13(Z)-4-bromobenzaldehyde oxime (2m). Isolation condition, Hexane: ethyl acetate (9:1), White crystalline solid(480mg, 90%),^{1}H NMR (400 MHz, $CDCl_3$) δ 8.27 (s, 1H), 8.10 (s, 1H), 7.55 – 7.49 (m, 2H), 7.46 – 7.39 (m, 2H).^{13}C NMR (101 MHz, $CDCl_3$) δ 149.43, 132.06, 130.87, 128.46, 124.32, 77.36, 77.04, 76.72, HRMS (ESI): Calculated for C_7H_6BrNO $[M+H]^+$: 199.9633, found 199.9679

4.2.2.14 (Z)-O-(4-((hydroxyimino)methyl)-3-methoxyphenyl) dimethyl carbamothioate (2n). Isolation condition, Hexane: ethyl acetate (7:3), White crystalline solid(840mg, 90.71%),^{1}H NMR (400 MHz, $CDCl_3$) δ 8.71 (s, 1H), 8.12 (s, 1H), 7.28 (d, *J* = 1.7 Hz, 1H), 7.11 (dd, *J* = 8.2, 1.8 Hz, 1H), 7.06 (d, *J* = 8.1 Hz, 1H), 3.84 (s, 3H), 3.45 (s, 3H), 3.35 (s, 3H). ^{13}C NMR (101 MHz, $CDCl_3$) δ 187.43, 151.90, 149.78, 144.31, 130.78, 124.33, 120.59, 109.87, 77.45, 77.14, 76.82, 56.07, 43.43, 38.84, HRMS (ESI): Calculated for $C_{11}H_{14}N_2O_3S$ $[M+H]^+$: 255.0725, found 255.0798.

4.2.2.15(Z)-4-(dimethylamino)benzaldehyde oxime (2o). Isolation condition, Hexane: ethyl acetate (9:1), Light yellow crystalline solid(500mg, 86%),^{1}H NMR (400 MHz, $CDCl_3$) δ 8.79 (s, 1H), 8.06 (s, 1H), 7.45 (d, *J* = 8.8 Hz, 2H), 6.68 (d, *J* = 8.8 Hz, 2H), 2.99 (s, 6H). ^{13}C NMR (101

MHz, $CDCl_3$) δ 151.56, 150.45, 128.34, 119.64, 111.95, 77.08, 40.25, HRMS (ESI): Calculated for $C_9H_{12}N_2O$ $[M+H]^+$: 165.0950, found 165.1008.

4.2.2.16(Z)-2-nitrobenzaldehyde oxime (2p). Isolation condition, Hexane: ethyl acetate (8:2), Light yellow crystalline solid(598mg, 85%),^{1}H NMR (400 MHz, $CDCl_3$) δ 8.69 (s, 1H), 8.12 (s, 1H), 8.07 (dd, *J* = 8.2, 1.1 Hz, 1H), 7.92 (dd, *J* = 7.8, 1.5 Hz, 1H), 7.69 – 7.62 (m, 1H), 7.56 (ddd, *J* = 8.2, 7.6, 1.5 Hz, 1H). ^{13}C NMR (101 MHz, $CDCl_3$) δ 147.08, 133.58, 130.44, 128.83, 127.16, 124.88, 77.35, 77.03, 76.72, HRMS (ESI): Calculated for $C_7H_6N_2O_3$ $[M+H]^+$: 167.0378, found 167.0448.

4.2.2.17(Z)-4-nitrobenzaldehyde oxime (2q). Isolation condition, Hexane: ethyl acetate (8:2), Light yellow crystalline solid (571mg, 85%),^{1}H NMR (400 MHz, $CDCl_3$) δ 8.27 (d, *J* = 8.6 Hz, 2H), 8.23 (s, 1H), 7.98 (s, 1H), 7.77 (d, *J* = 8.6 Hz, 2H). ^{13}C NMR (101 MHz, $CDCl_3$) δ 148.51, 148.40, 138.16, 127.68, 124.08, 77.35, 77.03, 76.72, HRMS (ESI): Calculated for $C_7H_6N_2O_3$ $[M+H]^+$: 167.0378, found 167.0449.

4.2.2.18(Z)-4-((hydroxyimino)methyl)benzonitrile (2r). Isolation condition, Hexane: ethyl acetate (8.5:1.5), Bright needle crystalline solid (574mg, 89%), ^{1}H NMR (400 MHz, DMSO) δ 11.74 (s, 1H), 8.24 (s, 1H), 7.86 (d, *J* = 6.7 Hz, 2H), 7.78 (d, *J* = 1.7 Hz, 2H). ^{13}C NMR (101 MHz, DMSO) δ 147.59, 138.08, 133.14, 127.48, 119.17, 111.84, 40.59, 40.38, 40.17, 39.96, 39.75, 39.54, 39.33, HRMS (ESI): Calculated for $C_7H_6N_2O_3$ $[M+H]^+$: 147.0480, found 147.0514.

4.2.2.19(Z)-1H-indole-3-carbaldehyde oxime (2s). Isolation condition, Hexane: ethyl acetate (7:3), Light yellow solid (359mg, 85%), ^{1}H NMR (400 MHz, DMSO) δ 11.40 (s, 1H), 10.52 (s, 1H), 8.29 (s, 1H), 8.00 (d, *J* = 7.9 Hz, 1H), 7.63 (d, *J* = 2.7 Hz, 1H), 7.45 – 7.41 (m, 1H), 7.20 – 7.15 (m, 1H), 7.13 – 7.07 (m, 1H). ^{13}C NMR (101 MHz, DMSO) δ 145.09, 137.35, 128.85, 124.71, 122.75, 121.94, 120.50, 112.24, 110.09, 40.59, 40.38, 40.17, 39.97, 39.76, 39.55, 39.34, HRMS (ESI): Calculated for $C_9H_8N_2O$ $[M+H]^+$: 161.0637, found 161.0687.

4.2.2.20 (Z)-heptanal oxime (2t). Isolation condition, Hexane: ethyl acetate (9:1), Liquid (400mg, 46%),^{1}H NMR (400 MHz, $CDCl_3$) δ 7.95 (s, 1H), 6.72 (t, *J* = 5.5 Hz, 1H), 2.38 (td, *J* = 7.5, 5.5 Hz, 2H), 1.54 – 1.44 (m, 2H), 1.39 – 1.25 (m, 6H), 0.92 – 0.87 (m, 3H). ^{13}C NMR (101 MHz, $CDCl_3$) δ 153.02, 77.34, 77.23, 77.03, 76.71, 31.51, 29.04, 26.02, 24.97, 22.53, 14.03, HRMS (ESI): Calculated for $C_7H_{15}NO$ $[M+H]^+$: 130.1154, found 130.1187.

4.2.2.21(Z)-Octanal oxime (2u): ^{1}H NMR (400 MHz, $CDCl_3$) δ 9.92 (s, 1H), 9.92 (s, 1H), 7.75 (d, *J* = 9.5 Hz, 1H), 7.75 (d, *J* = 9.5 Hz, 1H), 6.20 – 5.98 (m, 2H), 6.19 – 5.98 (m, 2H), 2.16 (dd, *J* = 14.2, 7.2 Hz, 2H), 1.47 – 1.36 (m, 2H), 1.35 – 1.20 (m, 6H), 0.89 (t, *J* = 6.8 Hz, 3H).^{13}C NMR (101 MHz, $CDCl_3$) δ 151.82, 143.02, 123.63, 77.41, 77.09, 76.77, 32.93, 32.78, 31.63, 28.81, 28.61, 28.46, 14.03.

4.2.2.22(Z)-2-Methyl prapanal oxime (2v): ^{1}H NMR (400 MHz, $CDCl_3$) δ 7.47 (s, 1H), 3.36 (d, *J* = 2.8 Hz, 1H), 2.01 – 1.90 (m, 1H), 1.17 (d, *J* = 17.1 Hz, 6H).^{13}C NMR (101 MHz, $CDCl_3$) δ 158.22, 81.99, 77.34, 77.02, 76.71, 41.67, 29.30, 24.30, 22.60, 22.49, 16.59.

5. Biological and computational study

5.1. In silico study

5.1.1. Molecular docking studies of ***2d*** *(p-Methoxy benzyl oxime) and* **2g** *(2,3,4-Trimethoxybenzyl oxime)*

PDB structure of MRCK kinase was downloaded from PDB (ID: 5OTE) isolated from Escherichia coli. The obtained structure of the protein is made of 419 amino acid and the active site of the enzyme was determined using an online server CASTp http://sts.bioe.uic.edu/castp/index.html?j_5d6259eb0df35. Active site of the enzyme was recognized with surface area of 573.84 and volume of 546.66. The 3D structure of the 2d and 2g were drawn and validated using ChemBioDrwa (3D). Windows based docking tool Autodock 4.2.6 was used for docking study. Discovery studio visualizer was used to analyze the molecular interactions between docked molecules with MRCK Kinase. Autodock 4.2.6 tool used for molecular docking study. Docking analysis was initiated with the blind docking followed by site specific docking to find out the best-fit protein-ligand docked model for the Tamoxifen and **2d** and **2g**. All water molecules of MRCK kinases were removed and polar hydrogen atoms and Gasteiger charges were added. Interaction between MRCK Kinase protein and compound 2d and 2g are respected GLN (144), VAL (35), ASP(32) and VAL (35), GLN (144), HIS (395), LYS (109), GLN (70) (Figure 2.).

5.1.2 Invitro study

5.1.3. Experimental

Nine cancer cell lines were used for testing the prepared oximes viz. A431 (human epidermoid carcinoma cell line); A549 (adenocarcinomic human alveolar basal epithelial cells); L-132 (Human lung cells carcinoma).; NCI-H 460 (non-small-cell lung cancer cell lines); NCI-H520 (non-small cell lung carcinoma cell lines); PC3 (PC-3) is a human prostate cancer cell line; HepG2 (human liver cancer cell line); MDA-MB-231 (epithelial, human breast cancer cell line);.MCF-7 (b The RPMI & DMEM media, trypsin, antibiotic-antimycotic (Ab/Am) solution, Sodium bicarbonate, HEPES and MTT dye were purchased from Sigma-Aldrich, India. The fetal bovine serum was obtained from Gibco-BRL, India. The 96-well plates, T-25 and T-75 flasks were procured from Nunc, Thermo-Fisher Scientific, and India. DMSO and ethanol were purchased from Merck Pvt. Ltd., India.

The compounds were tested against a set of of cancer cell lines including MCF-7, A431, A549, PC-3, HepG2, MDAMB-231, L-132, NCIH-520, NCIH-460 procured from the National Centre for Cell Science (NCCS), Pune, India. The antiproliferative potential of the synthesized compounds was evaluated by employing MTT assay and the experiments were performed by following the method reported previously[42]. In brief, the cells were grown in a CO_2 incubator at 37°C and 85% humidity in media supplemented with 1 % Ab/Am and 10 % FBS. Experimentally, the cells were seeded in a 96-well flat bottom plate and incubated for 24h. After incubation, the cells were treated with compounds at different concentrations (0.4-50µg/mL) and further incubated for 24 h. The MTT dye was added and then plate was incubated for 4 h at 37°C in dark. After that, the dye was removed and DMSO was added to dissolve the formazan crystals followed by recording of absorbance at 570nm. Tamoxifen was used as a standard. The percent cytotoxicity and inhibitory concentration (IC_{50}) was calculated as reported previously [43] (Table 4, Fig 1). reast cancer cell line).

5.1.3. Cell cycle analysis

Cell cycle analysis was performed to check the effect of compound (**2g** and **2d**) in a different phase of the cell cycle in. The cell lines A431 and NCIH-460 were treated with the compound **2g** and **2d** at IC_{50} and double of IC_{50} concentrations. The PI staining method was used as reported previously [44]. The cells (A431 and NCIH-460) were seeded in 6 well plates and incubated for 24h. After incubation, the cells were treated with the compounds for 24h at 37°C. After that, the cells were collected and fixed in 70% ice-cold ethanol. Afterward, the cells were

re-suspended in PBS and add DNA extraction buffer and further incubated for 5 min. After that, cells were centrifuged and re-suspended in the buffer and incubated with propidium iodide and RNAse A for 30 min in the dark at room temperature. The samples were analyzed by LSRII Flow-Cytometer (BD Biosciences).

5.1.4.Annexin V-FITC assay

The apoptosis assay was performed as per the reported protocol [45]. NCIH-460 cells were seeded in 6 well plates and incubated for 24h. The cells were treated with compounds 2g and 2d at different concentration (IC_{50} and double of IC_{50}) for 24h. After incubation, the cells were collected and washed with ice-cold PBS centrifuged for 5 min at 5000 rpm. The pellet was dissolved in 1x binding buffer, and the dyes FITC-annexin V and propidium iodide were added as per the manufacture protocol of BD Bioscience kit manual. The samples were incubated for 15 min, and after that analyzed by the LSRII Flow-Cytometer (BD Biosciences). The data were analyzed as reported earlier protocol [46].

5.1.5. Reactive oxygen species (ROS) assay

The ROS formation was determined by using DCFDA dye as per the protocol of Hamidullah et al., 2015. The NCIH-460 cells were seeded in 6 well plates for 24h. The cells were treated with the compound **2g** and **2d** at different concentration (IC_{50} and double of IC_{50}) for 24h. After incubation, the cells were collected and further incubate with DCFDA dye at room temperature for 30 min in the dark. After that, the cells were centrifuged at 5000 rpm and re-suspended in PBS. The samples were analyzed by using LSRII Flow-Cytometer (BD Biosciences).

5.1.6. Mitochondrial membrane potential

The mitochondrial membrane potential was measured using rhodamine 123 as per the method of Yu et al., 2015. The NCIH-460 cells were seeded in 6 well plates and incubated for 24 h. Different concentrations (IC_{50} and double of IC_{50}) of 2g and 2d were added and further incubated for 24h. After incubation, the cells were collected and treated with rhodamine dye at 37°C in the dark for 30 min. The cells were washed with PBS and re-suspended in PBS. The samples were analyzed by LSRII Flow-Cytometer (BD Biosciences).

6. Conclusion

An unexpected mild base catalyzed Michael type nucleophilic addition reaction followed with Retro-Knoevenagel reaction with aqueous hydroxylamine involving C-C bond cleavage in case of α -cyano substituted carbonyl conjugated and other similarly activated alkenes has been exploited for the formation of stereoselective aryl/alkyl oximes. The new procedure involves 1, 3 proton shift, Michael addition type reaction, followed by carbon-carbon bond cleavage resulting in elimination of ethyl cyanoacetate/ malononitrile/ dimethyl malonate. The yields of oximes were in the order heterocyclic>aryl>alkyl. Our new greener strategy presents one step and cost effective preparation of predominantly Z -oximes. Moreover, utility of carbon-carbon bond cleavage in the reaction, offered a great advantage in allowing water for the Michael addition to afford the corresponding oximes.

Out of the twenty two prepared Z-oximes two viz. p-Methoxy benzyl oxime and 2,3,4-Trimethoxy benzyl oxime were found to be cytotoxic in all the nine cancer cell lines used. The cell lines used were A431 (human epidermoid carcinoma cell line); A549 (adenocarcinomic human alveolar basal epithelial cells); L-132 (Human lung cells carcinoma).; NCI-H 460 (non-small-cell lung cancer cell lines); NCI-H520 (non-small cell lung carcinoma cell lines); PC3 (PC-3) is a human prostate cancer cell line; HepG2 (human liver cancer cell line); MDA-MB-231 (epithelial, human breast cancer cell line);. MCF-7 (breast cancer cell line). MIT, Cell cycle, Apoptotic, Reactive oxygen and Mitochondrial membrane assays were performed to evaluate the anticancer activity .These two oximes were found to inhibit MRCK Kinase, responsible for metastatic spread of cancer mortality.

Acknowledgements

This work was financially supported by the National Academy of Science India, (Senior Scientist Grant), Allahabad.

References

[1] M. Murakami and T. Matsuda, Metal-catalysed cleavage of carbon–carbon bonds. Chem. Com. 47 (2011) 1100–1105.

[2] (a) M. Tobisu, H. Kinuta, Y. Kita, E. Rémond and N. Chatani, Rhodium (I)-Catalyzed Borylation of Nitriles through the Cleavage of Carbon–Cyano Bonds. J. Am. Chem. Soc. 134 (2012) 115–118. (b) L. Li and J. Zhang, Lewis Acid-catalyzed [3 + 2]Cyclo-addition of Alkynes with N-Tosyl-aziridines via Carbon–Carbon Bond Cleavage: Synthesis of Highly Substituted 3-Pyrrolines. Org. Lett. 13 (2011) 5940–5943. (c) H. Li, Y. Li, X. S. Zhang, K. Chen, X. Wang and Z. J. Shi, Pyridinyl Directed Alkenylation with Olefins via Rh(III)-Catalyzed C–C Bond Cleavage of Secondary Arylmethanols. J. Am. Chem. Soc.133 (2011) 15244–15247. (d) D. E. Herbert, J. B. Gilroy, A. Staubitz, M. F. Haddow, J. N. Harvey and I. Manners, Strain-Induced Cleavage of Carbon−Carbon Bonds: Bridge Rupture Reactions of Group 8 Dicarba[2]metallocenophanes. J. Am. Chem. Soc. 132 (2010) 1988–1998.

[3] (a) K. Miyamoto, N. Tada and M. Ochiai, Activated Iodosylbenzene Monomer as an Ozone Equivalent: Oxidative Cleavage of Carbon−Carbon Double Bonds in the Presence of Water. J. Am. Chem. Soc. 129 (2007) 2772–2773. (b) R. Lin, F. Chen and N. Jiao, Metal-Free, NHPI Catalyzed Oxidative Cleavage of C–C Double Bond Using Molecular Oxygen as Oxidant. Org. Lett. 14 (2012) 4158–4161.(c) A. Sattler and G. Parkin, Cleaving carbon–carbon bonds by inserting tungsten into unstrained aromatic rings. Nature 463 (2010) 523–526.

[4] (a) T. Shen, T. Wang, C. Qin and N. Jiao, Silver□Catalyzed Nitrogenation of Alkynes: A Direct Approach to Nitriles through C□C Bond Cleavage. Angew. Chemie - Int. Ed. 52 (2013) 6677–6680.(b) A. Wang and H. Jiang, Palladium-Catalyzed Cleavage Reaction of Carbon−Carbon Triple Bond with Molecular Oxygen Promoted by Lewis Acid. J. Am. Chem. Soc. 15 (2008) 5030–5031. (c) L. J. Wang, H. T. Zhu, L. Lu, F. Yang, X. Y. Liu and Y. M. Liang, Highly Regioselective Synthesis of 1,3-Diiodonaphthalene Derivatives via a Sequential Cascade Iodocyclization. Org. Lett. 14 (2012) 1990–1993.

[5] G. W. Huber, S. Iborra and A. Corma, Synthesis of Transportation Fuels from Biomass: Chemistry, Catalysts, and Engineering. Chem. Rev. 106 (2006) 4044–4098.

[6] M. Tobisu and N. Chatani, Catalytic reactions involving the cleavage of carbon–cyano and carbon–carbon triple bonds. Chem. Soc. Rev. 37 (2008) 300–307.

[7] E. Lourdusamy, L. Yao, and C.-M. Park, Stereoselective Synthesis of a-Diazo Oxime Ethers and Their Application in the Synthesis of Highly Substituted Pyrroles through a [3+2] Cycloaddition. Angew. Chem. Int. Ed. 49 (2010) 7963 –7967.

[8] S. Emami, M. Falahati, A. Banifatemib and A. Shafiee, Stereoselective synthesis and antifungal activity of (Z)-trans-3-azolyl-2-methylchromanone oxime ethers Bioorg. Med. Chem. 12 (2004) 5881–5889.

[9] B. A. Mendelsohn, S. Lee, S. Kim, F. Teyssier, V. S. Aulakh and M. A. Ciufolini, Oxidation of Oximes to Nitrile Oxides with Hypervalent Iodine Reagents. Org. Lett. 11 (2009) 1539–1542.

[10] N. A. Owston, A. J. Parker and J. M. J. Williams, Highly Efficient Ruthenium-Catalyzed Oxime to Amide Rearrangement. Org. Lett. 9 (2007) 3599–3601.

[11] (a) P. Chaudhuri, Homo-and hetero-polymetallic exchange coupled metal-oximates. Coord. Chem. Rev. 243 (2003) 143–190. (b) V. Y. Kukushkin and A. J. L. Pombeiro, Oxime and oximate metal complexes: unconventional synthesis and reactivity. Coord. Chem. Rev. 181 (1999) 147–175. (c) V. Y. Kukushkin, D. Tudela and A. J. L. Pombeiro, Metal-ion assisted reactions of oximes and reactivity of oxime-containing metal complexes. Coord. Chem. Rev. 156 (1996) 333–362.

[12] G. L. Kad, M. Bhandari, J. Kaur, R. Ratheea and J. Singha, Solventless preparation of oximes in the solid state and via microwave irradiation. Green Chem. 3 (2001) 275-277

[13] S. Sasatani, T. Miyazaki, K. Maruoka and H. Yamamoto, Diisobutylaluminum hydride: a novel reagent for the reduction of oximes. Tetrahedron Lett. 24 (1983) 4711–4712.

[14] G. M. Robertoson, In Comprehensive Functional Group Transformation, A. R. Katritzky, O. Meth-Cohn, Rees, C.W. Eds.; Elsevier, Oxford 3 (1995) 425.

[15] Y. Takahashi, Y. Miyashita, Y. Tanaka, H. Abe and S. ichi Sasaki, A consideration for structure-taste correlations of perillartines using pattern-recognition techniques. J. Med. Chem. 25 (1982) 1245–1248.

[16] P. A. Eyer, F. Worek, In Chemical Warfare Agents Toxicology and Treatment; T.C. Marrs, R. L. Maynard, F. R. Sidell, Eds. Wiley. (2007) 305–329.

[17] (a) J. P. Ley and H. J. Bertram, Catecholoximes as powerful antioxidants for highly unsaturated lipids. Eur. J. Lipid Sci. Technol., 2002, 104, 319–323.(b) M. Kato, S. Nishino, M. Ohno, S. Fukuyama, Y. Kita, Y. Hirasaw, I. Nakanishi, H. Takasugi and K. Sakane, New reagents for controlled release of nitric oxide. Structure-stability relationships. Bioorganic Med. Chem. Lett. 6 (1996) 33–38.

[18] R. W. Hartmann, M. Hector, S. Haidar, P. B. Ehmer, W. Reichert and J. Jose, Synthesis and evaluation of novel steroidal oxime inhibitors of P450 17 (17α-hydroxylase/C17− 20-lyase) and 5α-reductase types 1 and 2. J. Med. Chem. 43 (2000) 4266–4277.

[19] A. Pohjakallio and P. M. Pihko, Enantioselective Synthesis of 2□Isoxazolines by a One□Flask Conjugate Addition/Oxime□Transfer Process. Chem. - A Eur. J. 15 (2009) 3960–3964.

[20] C. L. Allen, S. Davulcu and J. M. J. Williams, Catalytic acylation of amines with aldehydes or aldoximes. Org. Lett. 12 (2010) 5096–5099.

[21] K. Johnson and E. F. Degering, The utilization of aliphatic nitro compounds.(I) The production of amines and (II) The production of oximes. J. Am. Chem. Soc. 61 (1939) 3194–3195.

[22] M. T. Schümperli, C. Hammond and I. Hermans, Developments in the aerobic oxidation of amines. ACS Catal. 2 (2012) 1108–1117.

[23] K. Suzuki, T. Watanabe and S. I. Murahashi, Oxidation of Primary Amines to Oximes with Molecular Oxygen using 1,1-Diphenyl-2-picrylhydrazyl and WO3/Al2O3 as Catalysts. J. Org. Chem. 78 (2013) 2301–2310.

[24] K. Suzuki, T. Watanabe and S. I. Murahashi, Aerobic Oxidation of Primary Amines to Oximes Catalyzed by DPPH and WO3/Al2O3. Angew. Chemie - Int. Ed. 47 (2008) 2079–2081.

[25] N. Kapuriya, K. Kapuriya, N. M. Dodia, Y. W. Lin, R. Kakadiya, C. T. Wu, C. H. Chen, Y. Naliapara and T. L. Su, Novel oxidative nitrogen to carbon rearrangement found in the conversion of anilines to benzaldoximes by treating with HCHO/H2O2. Tetrahedron Lett. 49 (2008) 2886–2890.

[26] X. Xue, F. Song, B. Ma, Y. Yu, C. Li and Y. Ding, Selective ammoximation of ketones and aldehydes catalyzed by a trivanadium-substituted polyoxometalate with H2O2 and ammonia. Catal. Commun. 33 (2013) 61–65.

[27] D. Sloboda-Rozner and R. Neumann, Aqueous biphasic catalysis with polyoxometalates: oximation of ketones and aldehydes with aqueous ammonia and hydrogen peroxide. Green Chem. 8 (2006) 679–681.

[28] R. B. Silverman, Radical ideas about monoamine oxidase. Acc. Chem. Res. 28 (1995) 335–342.

[29] S. I. Murahashi and D. Zhang, Ruthenium catalyzed biomimetic oxidation in organic synthesis inspired by cytochrome P-450. Chem. Soc. Rev. 37 (2008) 1490–1501.

[30] N. Fischer, D. Fischer, T. M. Klapötke, D. G. Piercey and J. Stierstorfer, Pushing the limits of energetic materials – the synthesis and characterization of dihydroxylammonium 5,5′-bistetrazole-1,1′-diolate. J. Mater. Chem. 22 (2012) 20418–20422.

[31] Q. Hua-Li, L. Jing, Z. Cheng-Pan, J. Ibrahim, A. M. Wahab, S. Muhammad, N.-ul-H. Muhammad, A. H. Muhammad and N. A. B. Syed, Synthesis of α, β-unsaturated carbonyl-based compounds, oxime and oxime ether analogs as potential anticancer agents for overcoming cancer multidrug resistance. J. Med. Chem. 59 (2016) 3549-3561.

[32] Q. Zhang, J. Dong, J. Cui, G. Huang, Q. Meng, S. Li, Cytotoxicity of Synthesized 1,4-Naphthoquinone Oxime Derivatives on Selected Human Cancer Cell Lines. Chemical and Pharmaceutical Bulletin, 66 (2018) 612-619.

[33] S.-J. Choi, J.-E. Lee, S.-Y. Jeong, I. Isak, S.-D. Lee, E.-J. Lee, S. K. Lee, S.-M. Kwon, S.-G. Ahn, J.-H. Yoon, S.-Y. Han, J.-I. Kim and Y. –C. Kim, 5, 5′-substituted indirubin-3′-oxime derivatives as potent cyclin-dependent kinase inhibitors with anticancer activity. J. Med. Chem. 53 (2010) 3696-3706.

[34] H.-L. Qin, J. Leng, C.-P. Zhang, I. Jantan, M. W. Amjad, M. Sher, M. N.-ul-Hassan, M. A. Hussain and S. N. A. Bukhari, Synthesis of α,β-Unsaturated Carbonyl-Based Compounds, Oxime and Oxime Ether Analogs as Potential Anticancer Agents for Overcoming Cancer

Multidrug Resistance by Modulation of Efflux Pumps in Tumor Cells. J. Med. Chem. 59 (2016) 3549-3561.

[35] Ken□Ming Chang, Li□Chai Chen, Cherng□Chyi Tzeng, Yao□Hua Lu, I□Li Chen, Shin□Hun Juang, Tai□Chi Wang, Synthesis and antiproliferative evaluation of oxime, methyloxime, and amide□containing quinazolinones. J. Chin. Chem. Soc. 65 (9) (2018) 1110–1118.

[36] A. Hall, The cytoskeleton and cancer. Cancer Metastasis Rev. 28 (2009) 5–14.

[37] M. F. Olson and E. Sahai, The actin cytoskeleton in cancer cell motility. Clin. Exp. Metastasis. 26 (2009) 273–87.

[38] C. Gaggioli, S. Hooper, C. Hidalgo-Carcedo, R. Grosse, J. F. Marshall and K. Harrington, Fibroblast-led collective invasion of carcinoma cells with differing roles for RhoGTPases in leading and following cells. Nat. Cell. Biol. 9 (2007) 1392–400.

[39] M. Unbekandt, D. R. Croft, D. Crighton, M. Mezna, D. McArthur and P. McConnell P, A novel small-molecule MRCK inhibitor blocks cancer cell invasion. Cell Commun. Signal. 12 (2014) 54.

[40] E. Bremer, G. van Dam, B. J. Kroesen, L. de Leij and W. Helfrich, In Situ Detection of Apoptosis by the TUNEL Assay: An Overview of Techniques. Trends Mol Med. 12 (2006) 382-93.

[41] S. Singh, V. Dubey, D. K. Singh, K. Fatima, A. Ahmad and S. Luqman, Antiproliferative and antimicrobial efficacy of the compounds isolated from the roots of Oenothera biennis L. Journal of Pharmacy & Pharmacology 69 (9) (2017) 1230 -1243.

[42] P. Maurya, S. Singh, M.M. Gupta and S. Luqman, Characterization of bioactive constituents from the gum resin of Gardenia lucida and its pharmacological potential. Biomedicine & Pharmacotherapy 85 (2017) 444–456.

[43] S.D. Kapkoti, S. Singh, S. Luqman and S.R. Bhakuni, Synthesis of novel 1, 2, 3-triazole based artemisinin derivatives and their antiproliferative activity. New J. Chem. 42 (2018) 5978-5995.

[44] S. Khwaja, K. Fatima, Hassanain, C. Behera, A. Kour, A. Singh, S. Luqman, J. Sarkar, D. Chanda, K. Shanker, A.K. Gupta, D.M. Mondhe and A. S. Negi, Antiproliferative efficacy of curcumin mimics through microtubule destabilization. Eur. J. Med. Chem. 151 (2018) 51–61.

[45] Hamidullah, K. S. Saini, N. Devender, A. Bhattacharjee, S. Das, S. Dwivedi, M. P. Gupt, H. K. Bora, K. Mitra, R. P. Tripathi, R. Konwar. Triazole analog 1-(1-benzyl-5-(4-chlorophenyl)-1H-1,2,3-triazol-4-yl)-2-(4-bromophenylamino)-1-(4 chlorophenyl)ethanol induces reactive oxygen species and autophagy-dependent apoptosis in both in vitro and in vivo breast cancer models. Int. J. Biochem. Cell. Biol. 65 (2015) 275.

Table 1: Optimization of the reaction conditions

Entry	Base	Time(h)	Solvent	Temp. (˚C)	Yield (%)[b]
1.	Na_2CO_3	1	MeOH	60	-
2.	Na_2CO_3	1	EtOH	70	-
3.	Na_2CO_3	1	THF	70	-
5.	Na_2CO_3	1	DMF	100	-
6.	Na_2CO_3	1	DMSO	100	-
7.	**Na_2CO_3**	**1**	**MeOH/Water[a]**	**100**	**92[b]**
8.	Na_2CO_3	1	EtOH / Water[a]	100	86
9.	Na_2CO_3	1	THF/ Water[a]	100	56
10.	Na_2CO_3	1	DMSO/Water[a]	100	67
11.	Na_2CO_3	1	Water	100	45
12.	Na_2CO_3	4	MeOH/Water[a]	rt	90

Note: a Solvent / water (9:1), b Isolated yield.

Table 2: Impact of base on yield of benzyl oxime.

Entry	Base	Time (h)	Temperature (°C)	Solvent:water (9:1)	Yield (%)
1.	DABCO	1	100	MeOH : Water	68
2.	TEA	1	100	MeOH : Water	66
3.	K_2CO_3	1	100	MeOH : Water	90
4.	Na_2CO_3	1	100	MeOH : Water	92
5.	DBU	1	100	MeOH : Water	88
6.	NaOH	1	100	MeOH : Water	75
7.	KOH	1	100	MeOH : Water	74

Note: Reaction condition: Ethyl (*E*)-2-cyano-3-phenyl (4.9 mmol), hydoxylamine hydrochloride (5.97 mmol), Base (5.97 mmol), 100 °C, 1h.

Table 3: Substrate scope of oximes.

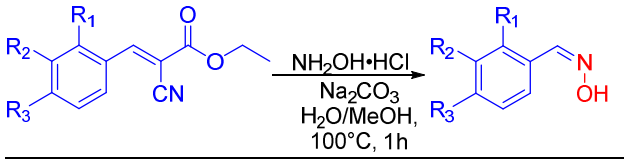

2a, 92, R_1=R_2=R_3=H
2b, 84, R_1=R_2=H, R_3=OH
2c, 77, R_1=H, R_2=R_3=OH
2d, 85, R_1=R_2=H, R_3= OCH_3
2e, 89, R_1=R_3=H, R_2= CH_3
2f, 87, R_1 =H, R_2=R_3= OCH_3
2g, 88, R_1=R_2=R_3= OCH_3
2h, 86, R_1=H, R_2= OCH_3, R_3=OH
2j, 92, R_1=R_2=H, R_3= F
2k, 88, R_1=Cl, R_2=R_3=H
2l, 88, R_1=H, R_2=Cl, R_3=H
2m, 90, R_1=R_2=H, R_3=Br
2o, 86, R_1=R_2=H, R_3= $(CH_3)_2NH$
2p, 85, R_1= NO_2, R_2=R_3=H
2q, 85, R_1=R_2=H, R_3=NO_2
2r, 89, R_1=R_2=H, R_3=CN

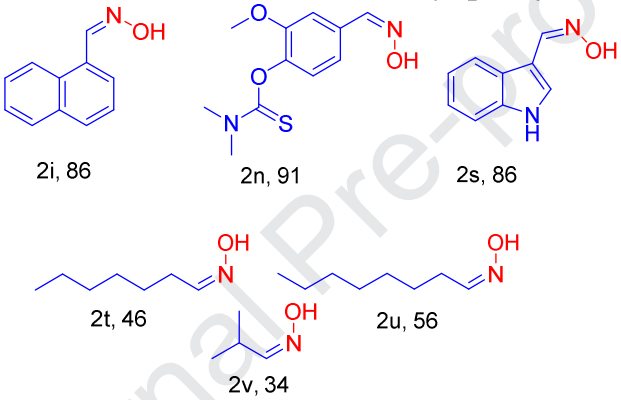

General reaction conditions: ethyl (E)-2-cyano-3-aryl/alkyl acrylate (4.9 mmol), hydoxylamine hydrochloride (5.97 mmol), sodium carbonate (5.97 mmol), 100 °C, 1h.

Table 4: IC_{50} value of synthesized compound for tested cell line.

Entry	A-431	A-549	L-132	NCIH-460	NCIH-520	PC-3	HepG-2	MDA-MB-231	MCF-7
2b	-	-	-	-	-	-	-	-	-
2c	-	-	-	-	-	-	-	-	-
2d	9.11±1.54	22.83±1.52	37.84±1.27	8.63±0.15	19.18±2.99	15.13±2.02	21.02±1.75	23.84±0.50	21.34±1.51
2e	-	-	-	-	-	-	-	-	-
2f	-	-	-	-	-	-	-	-	-
2g	10.24±0.90	12.53±0.96	44.26±0.39	9.42±0.39	16.15±0.69	14.94±0.91	16.44±0.29	17.66±0.67	18.75±3.39
2h	-	-	-	-	-	-	-	-	-
2i	12.25±0.40	24.49±1.27	28.69±0.86	22.29±1.08	-	18.39±2.10	-	21.76±0.94	23.09±3.73
2j	-	-	-	-	-	-	-	-	-
2k	40.80±1.55	-	-	-	-	-	-	-	-
2l	-	-	-	-	-	-	-	38.84±0.70	-
2m	-	-	-	-	-	-	-		-
2n	-	-	-	-	-	-	-	-	-
2o	-	-	-	-	-	-	-	-	-
2p	-	-	-	-	-	-	-	-	-
2q	-	-	-	-	-	-	-	-	-
2r	-	-	-	-	-	-	-	-	-

FIGURES

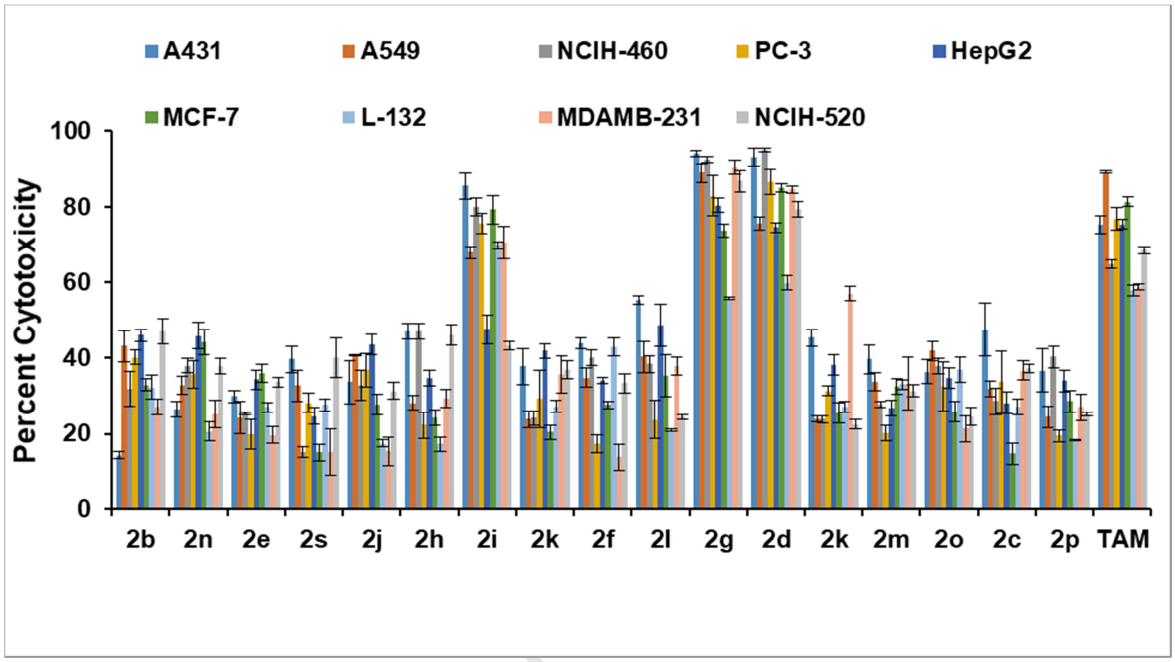

Figure 1: Percent cytotoxicity of synthetic oximes (2b-2p) vs standard drug Tamoxifen.

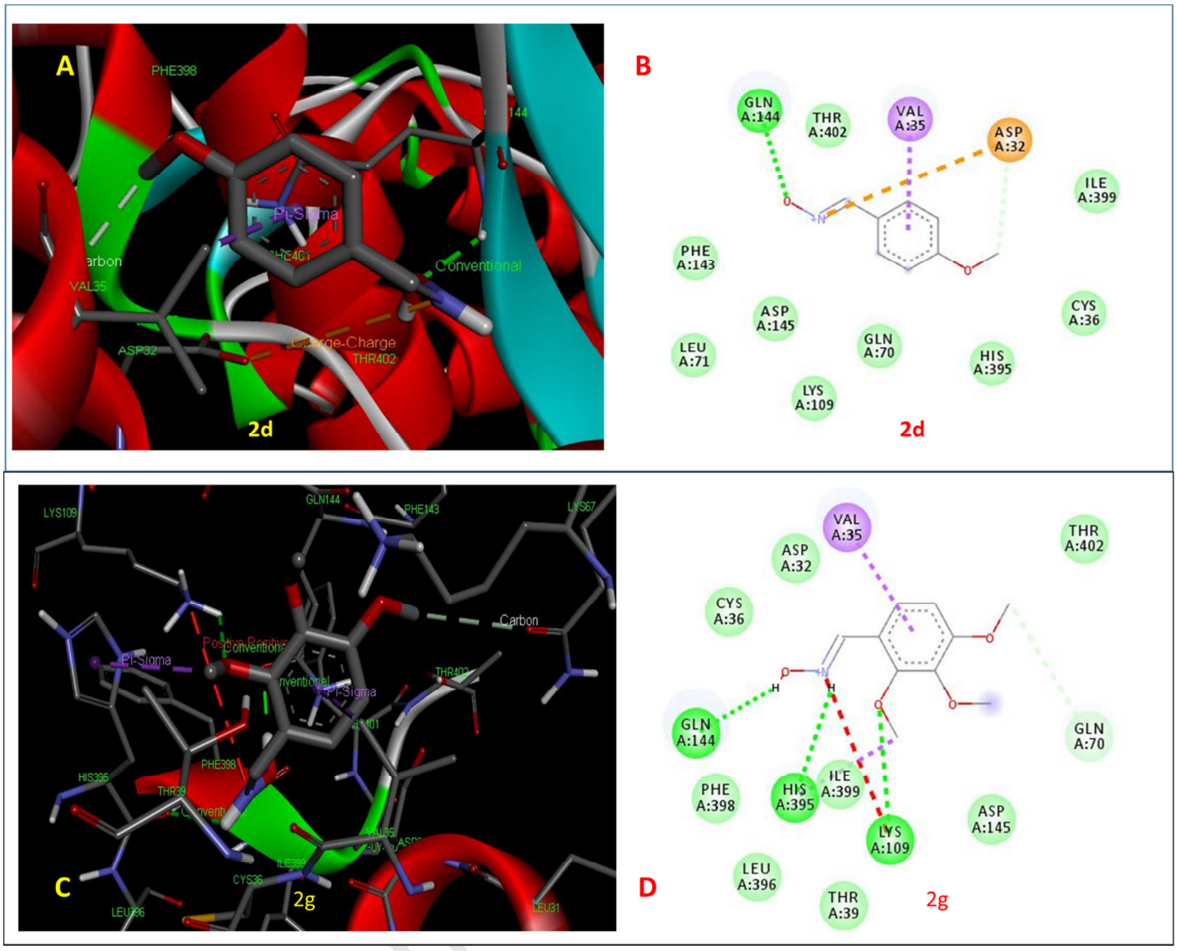

Figure 2: (A) Interaction of **2d** with MRCK Kinase (3D); (B) Interaction of **2d** with MRCK Kinase (2D); (C) Interaction of **2g** with MRCK Kinase (3D); (D) Interaction of **2g** with MRCK Kinase (2D).

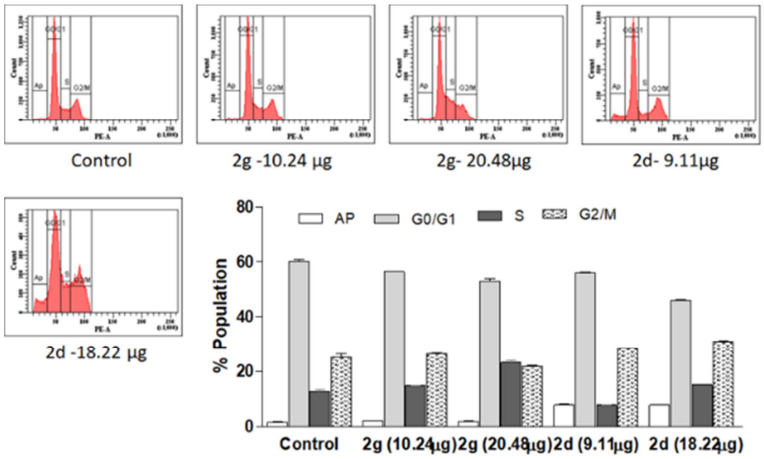

Figure 3: The effect of compound **2g** and **2d** in the A431 cell line on different phases of the cell cycle. The cell cycle analysis was performed by using propidium iodide (PI) staining. The pictorial graphs and percent population graphs are presented, and the pictorial graphs are one representative example of two experiments.

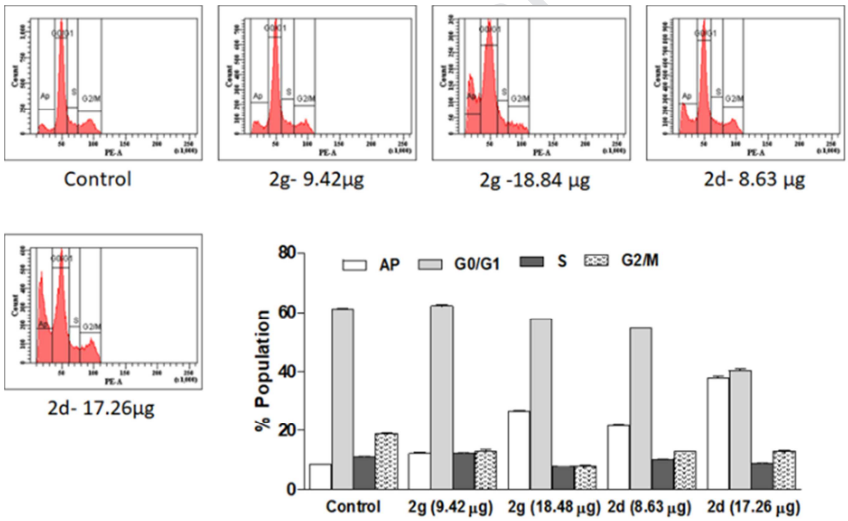

Figure 4: The effect of compound 2g and 2d in NCIH-460 cell line on different phases of the cell cycle. The cell cycle analysis was performed by using propidium iodide (PI) staining. The pictorial graphs and percent population graphs are presented, and the pictorial graphs are one representative example of two experiments.

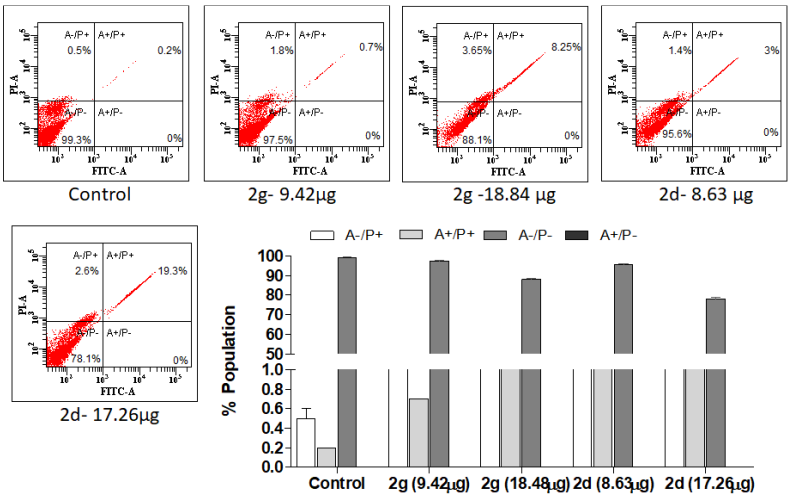

Figure 5: The apoptotic effect of compound 2g and 2d in NCIH-460 cell line. The apoptosis assay was performed by using Annexin-V-FITC staining. The pictorial graphs and percent population graphs are presented, and the pictorial graphs are one representative example of two experiments.

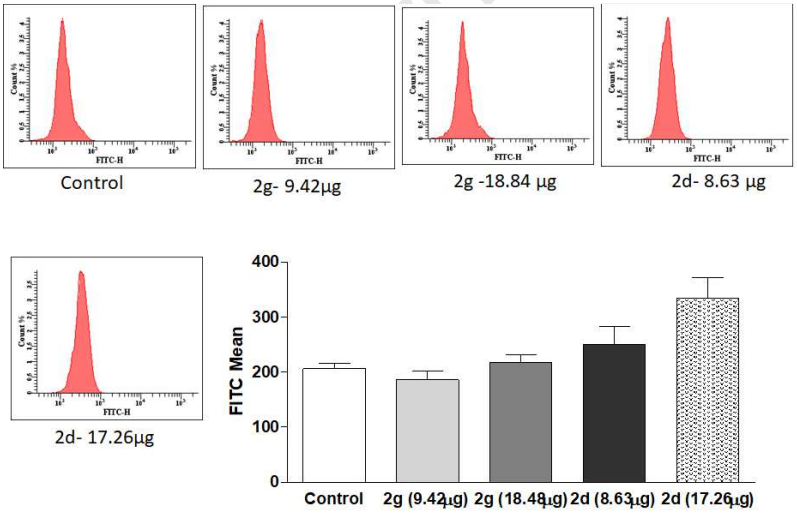

Figure 6: The ROS generation effect of compound 2g and 2d in NCIH-460 cell line. The reactive oxygen species (ROS) assay was performed by using DCFDA dye. The pictorial graphs and FITC mean graphs are presented, and the pictorial graphs are one representative example of two experiments.

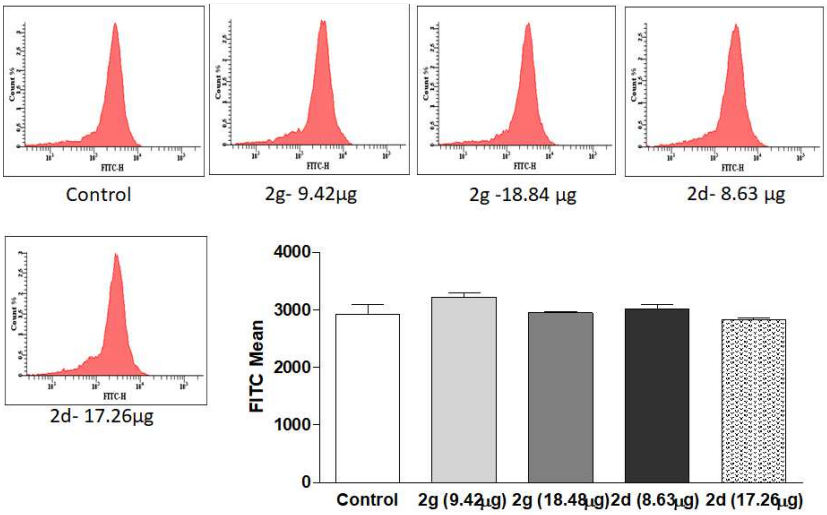

Figure 7: The effect of compound 2g and 2don mitochondrial membrane potential in NCIH-460 cell line. The mitochondrial membrane potential (MMP) assay was performed by using Rhodamine 123 dye. The pictorial graphs and FITC mean graphs are presented, and the pictorial graphs are one representative example of two experiments.

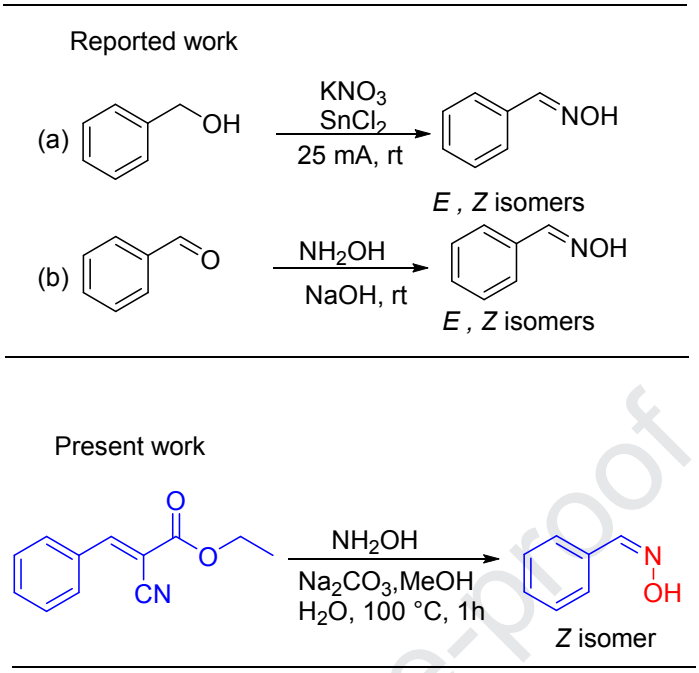

Scheme1: Conventional methods of synthesis of oximes yielding mixture of *E* & *Z* isomers and present method yielding predominantly *Z* isomer respectively.

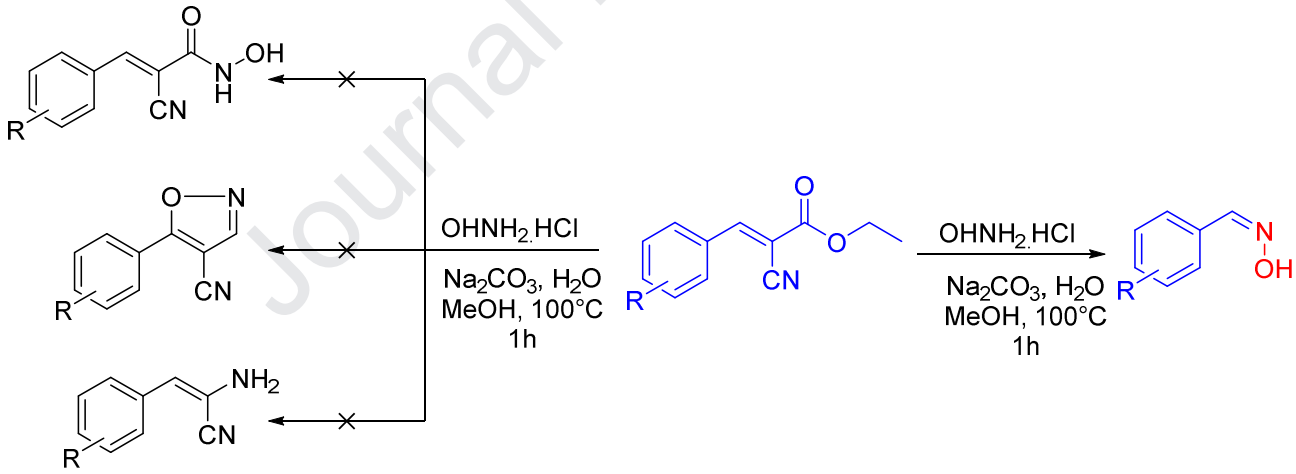

Scheme 2: Formation of oxime due to C-C bond cleavage.

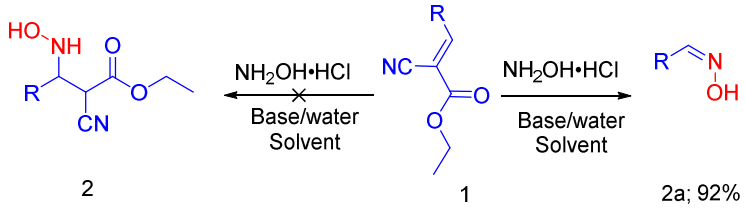

Scheme 3: Unexpected formation of benzyl oxime (2a)

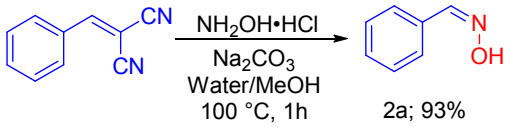

Scheme 4: Benzyl oxime (2a) from benzylidene malononitrile

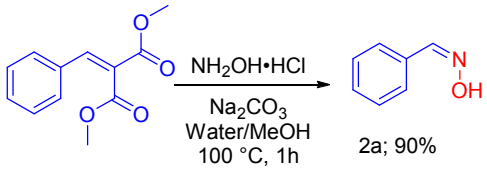

Scheme 5: Benzyl oxime (2a) from dimethyl-2-benzylidene malonate.

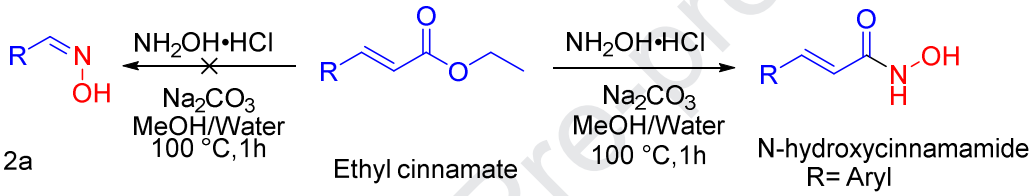

Scheme 6: Control experiment.

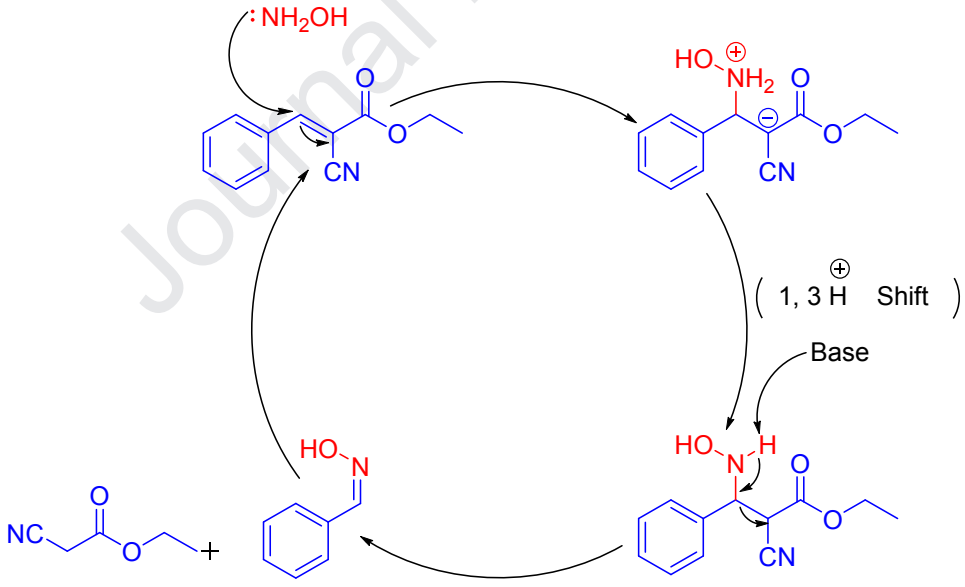

Scheme 7: a plausible mechanism is proposed for the synthesis of **2a**

Highlights

- Water mediated and base catalyzed C-C bond cleavage
- A novel and facile stereoselective strategy for synthesis of *Z* oximes
- Metal free, mild and time economic condition
- Good air and moisture tolerance broad substrate scope high stereoselective
- Small molecule inhibit MRCK kinase ,thereby may have good anticancer property

Conflict of Interest

Myself , Prof. Krishna Misra as corresponding author of this paper entitled, " Water mediated transition-metal-free-one pot cascade procedure for preparation of Stereoselective oximes as inhibitors of MRCK Kinase" wish to certify that there is no conflict of interest among the co authors.

Krishna Misra